

SUPPLEMENTARY DATA

ROI analysis: HOMA-IR and FDG metabolism associations in participants with MCI and AD enriched for amyloid positivity

Mild Cognitive Impairment and AD in the full cohort were defined exclusively on the basis of clinical and cognitive performance criteria. Here, we wish to refine our analyses by enriching MCI and AD participants for amyloid positivity. To this end, we searched for and downloaded all available baseline data for CSF A β ₄₂, Pittsburgh Compound B (PIB) scans, or AV45/Florbetapir scans. Of our original 280 participants, 177 had CSF A β ₄₂ values, an additional 34 participants had PIB scans, and an additional 17 participants had AV45 scans. In total, 227 out of 280 original participants had amyloid biomarker data. While plasma A β was available for an additional 48 participants, there is no clear cut-off in the literature for determining amyloid status.

We used the following cut-offs to determine amyloid-positivity for participants: CSF A β ₄₂ - values below 192 pg/mL; PIB - values above 1.4 mean Standardized Uptake Volume Ratio (SUVR) in frontal, parietal, and temporal areas normed to cerebellum; AV45 - values above 1.1 mean SUVR across frontal, temporal, precuneus, parietal, cortex, anterior cingulate, and posterior cingulate normed to cerebellum. The AV45-A11 study group determined this cut-off among these ROIs (Johnson et al., 2013). Decreasing the PIB threshold to a more liberal greater than 1.2 SUVR threshold changed amyloid status for only 2 participants. Thus, we used the more conventional cut-off. For the AD group, all 60 participants had amyloid data, and 54 participants were classified as amyloid-positive. For the MCI group, 141 out of 194 participants had amyloid data. By month 24, of these 141 MCI participants, 108 were MCI-S, 26 were MCI-P, and 7 were CN. The sample size breakdown for the MCI group by amyloid status at 24 months was as follows: MCI-S, amyloid-negative: 31; MCI-S, amyloid-positive: 77; MCI-P, amyloid-negative: 3; MCI-P, amyloid-positive: 23.

We then examined the main effects of HOMA-IR on FDG metabolism or its interaction effect with Baseline Diagnosis (CN vs. MCI vs. AD) or MCI Conversion (MCI-S vs. MCI-P) among our 5 ROIs (ventral prefrontal cortex, medial temporal lobe, hippocampus, posteromedial cortex, and lateral parietal cortex) and 2 control areas (global FDG, post-central gyrus). Covariates were identical to the main text analyses and included age, sex, education, diabetes status, APOE4 genotype status, and mean GM volume within each ROI to control for any partial volume effects. Given that these supplemental analyses were exploratory, alpha was set to .05.

Baseline diagnosis analysis

No significant main effects or interactions were found for control regions. For our 5 ROIs, similar to analyses in the full cohort, we found significant HOMA-IR * Baseline Diagnosis interactions for ventral prefrontal cortex [$F = 4.931$, $p = .027$], medial temporal lobe [$F = 4.868$, $p = .028$], hippocampus [$F = 5.228$, $p = .023$], posteromedial cortex [$F = 7.392$, $p = .007$], and lateral parietal cortex [$F = 7.104$, $p = .008$]. Simple slopes analyses indicated that only AD participants showed a significant association between HOMA-IR and FDG metabolism. For example, higher HOMA-IR predicted lower FDG metabolism in hippocampus ($R^2 = 0.150$, estimate = -0.084 , $p = .019$) and vPFC ($R^2 = 0.186$, estimate = -0.162 , $p = .005$). These results suggest that enriching for amyloid-positivity in MCI and AD did not influence the association between HOMA-IR and regional FDG-PET when considering baseline diagnosis.

SUPPLEMENTARY DATA

MCI conversion analysis

Similar to the analyses in the full MCI cohort, there were no main effects or interactions for the control areas, as well as for posteromedial cortex and lateral parietal cortex. For hippocampus [$F = 4.142$, $p = .044$], MTL [$F = 4.722$, $p = .032$], and vPFC [$F = 7.417$, $p = .008$], there were significant HOMA-IR * MCI Conversion interactions. Simple slopes analyses confirmed our existing findings. Specifically, higher HOMA-IR predicted more FDG metabolism in MCI-P for hippocampus ($R^2 = 0.134$, estimate = .089, $p = .016$) and MTL ($R^2 = 0.108$, estimate = .083, $p = .004$), while the MCI-S slopes were flat. Conversely, higher HOMA-IR predicted less FDG metabolism in MCI-S for PFC ($R^2 = 0.131$, estimate = -0.125, $p = .001$), while the MCI-P slope was positive but non-significant. These results suggest that amyloid-positivity did not influence the association between HOMA-IR and regional FDG metabolism in MCI participants who did or did not convert to AD 24 months after baseline. It is encouraging to note that despite the smaller sample size for MCI-P ($n=23$), HOMA-IR still predicted more FDG uptake exclusively in MTL regions.

We also investigated if amyloid status might modify the association between HOMA-IR and FDG uptake, by testing the HOMA-IR * Amyloid Status interaction for a given ROI. These analyses were restricted to the MCI-S sub-group, because it was the only group with sufficient numbers of amyloid-negative ($n=31$) and amyloid-positive ($n=77$) participants for analysis. None of the interactions among the 5 ROIs were significant, although the precuneus ROI showed a weak trend [$F = 2.787$, $p = .099$]. Despite these non-significant interactions, we examined on an exploratory basis the main effect of HOMA-IR on ROI FDG metabolism separately in MCI-S amyloid-negative and amyloid-positive participants. For PFC, amyloid-positive [$F = 11.400$, $p < .001$] but not amyloid-negative [$F = 0.057$, $p = .814$] MCI-S showed a negative association between HOMA-IR and FDG metabolism. In the main text, higher HOMA-IR was also significantly related to less FDG in all MCI-S participants. Results for MTL and hippocampus were non-significant for either amyloid status group. For posteromedial cortex, amyloid-positive [$F = 5.407$, $p = .023$] but not amyloid-negative [$F = 0.091$, $p = .767$] MCI-S participants showed a negative association between HOMA-IR and FDG metabolism [estimate = -0.123]. This result is in contrast to the non-significant MCI-S association collapsed across amyloid status in the main text. For lateral parietal cortex, amyloid-positive [$F = 4.951$, $p = .030$] but not amyloid-negative [$F = 0.211$, $p = .653$] MCI-S showed a negative association between HOMA-IR and FDG metabolism [estimate = -0.104]. Finally, to confirm that amyloid-positivity predicted less FDG metabolism, we also examined the main effect of amyloid status in MCI-S among the 5 ROIs. Amyloid-positive vs. amyloid-negative MCI-S had significantly lower FDG metabolism in PFC [$F = 8.482$, $p = .005$], MTL [$F = 5.045$, $p = .027$], hippocampus [$F = 6.201$, $p = .014$], posteromedial cortex [$F = 8.487$, $p = .005$], and lateral parietal cortex [$F = 8.074$, $p = .006$].

There are some limitations that should be noted with these supplementary analyses. Due to the design of ADNI, no amyloid data from CSF or PET was available for approximately 27% of the MCI group. There were also only 3 MCI-P and 6 AD cases that were amyloid-negative. Finally, the MCI-S amyloid-positive versus amyloid negative results are exploratory in nature and should be interpreted with caution. Thus, we can only draw conclusions for amyloid-positive AD and MCI participants, which are comparable to our conclusions from the full cohort reported in the main text.

SUPPLEMENTARY DATA

Supplementary Table 1. Main Effects of Diagnosis and HOMA-IR on ROI FDG Metabolism

Main Effect of Clinical Diagnosis				EIM ± SE				Pairwise Comparisons			
Region	Baseline Diagnosis		MCI Conversion		AD	MCI-S	MCI-P	MCI vs. CN	AD vs. CN	AD vs. MCI	MCI-P vs. MCI-S
	F value	p value	F value	p value							
Post-Central Gyrus	0.834	0.435 ^a	0.930	0.336 ^a	1.590 ± 0.069	1.566 ± 0.055	1.488 ± 0.088	-0.097	-0.079	-0.018	-0.076
Global Cerebrum FDG	7.061	0.001 ^a	1.654	0.200 ^a	1.125 ± 0.019	1.163 ± 0.016	1.134 ± 0.025	-0.064 ^{**}	-0.110 ^{***}	-0.047 ^{**}	-0.029
Lateral Parietal	6.718	0.001 ^b	3.464	0.065 ^b	1.195 ± 0.027	1.257 ± 0.022	1.199 ± 0.035	-0.075 [*]	-0.148 ^{***}	-0.073 ^{**}	-0.058
Precuneus + PCC	9.679	< 0.001 ^b	2.468	0.118 ^b	1.297 ± 0.028	1.366 ± 0.025	1.311 ± 0.039	-0.090 ^{**}	-0.183 ^{***}	-0.093 ^{***}	-0.055
Hippocampus	9.555	< 0.001 ^b	0.176	0.675 ^b	0.953 ± 0.014	1.004 ± 0.011	0.997 ± 0.018	-0.038 [*]	-0.088 ^{***}	-0.051 ^{***}	-0.007
MTL	4.688	0.010 ^b	0.275	0.601 ^b	0.940 ± 0.013	0.962 ± 0.011	0.970 ± 0.017	-0.042 ^{**}	-0.060 ^{**}	-0.018	-0.008
vPFC	6.058	0.003 ^b	1.881	0.172 ^b	1.164 ± 0.021	1.182 ± 0.018	1.192 ± 0.028	-0.079 ^{***}	-0.098 ^{**}	-0.020	-0.010

Main Effect of HOMA-IR				Model Estimates ± SE			
Region	Baseline Diagnosis		MCI Conversion		Baseline Diagnosis	MCI Conversion	MCI Conversion
	F value	p value	F value	p value			
Post-Central Gyrus	1.081	0.299 ^a	1.695	0.195 ^a	0.228 ± 0.220	-0.128 ± 0.098	-0.128 ± 0.098
Global Cerebrum FDG	2.358	0.126 ^a	2.358	0.126 ^a	-0.012 ± 0.008	-0.012 ± 0.008	-0.012 ± 0.008
Lateral Parietal	5.381	0.021 ^b	0.892	0.346 ^b	0.194 ± 0.084 [*]	-0.036 ± 0.038	-0.036 ± 0.038
Precuneus + PCC	5.425	0.021 ^b	0.579	0.448 ^b	0.213 ± 0.091 [*]	-0.033 ± 0.043	-0.033 ± 0.043
Hippocampus	7.824	0.006 ^b	0.174	0.677 ^b	0.124 ± 0.044 ^{**}	0.008 ± 0.020	0.008 ± 0.020
MTL	5.610	0.019 ^b	0.020	0.887 ^b	0.099 ± 0.042 [*]	-0.003 ± 0.019	-0.003 ± 0.019
vPFC	3.648	0.057 ^b	2.522	0.114 ^b	0.128 ± 0.067	-0.050 ± 0.025	-0.050 ± 0.025

SUPPLEMENTARY DATA

Fixed effect F statistics with corresponding levels of significance, followed by model parameter estimates and standard error (SE), from the mixed models for the ROIs. AD = Alzheimer's disease; CN = cognitively normal; FDG = Fluorodeoxyglucose; MCI = Mild Cognitive Impairment; HOMA-IR = Homeostatic Model Assessment of Insulin Resistance; MCI-P = MCI progressive; MCI-S = MCI stable; MTL = medial temporal lobe; PCC = posterior cingulate cortex; vPFC = ventral prefrontal cortex. * = $p \leq .05$, ** = $p \leq .01$, *** = $p \leq .001$.

^ABoth control regions (post-central gyrus, global cerebrum FDG uptake) were tested separately from ROIs. Holm-Bonferroni type 1 error correction required successive p values of .025 and .050 for any interactions to be considered significant.

^BFor each set of 5 ROIs per diagnostic group, Holm-Bonferroni type 1 error correction required successive p values of .010, .013, .017, .025, and .050 for interactions to be considered significant. Bold indicates significant p values and either pairwise comparisons or model estimates \pm SE.

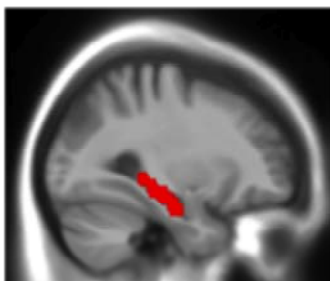
SUPPLEMENTARY DATA

Supplementary Figure 1. Regions of Interest

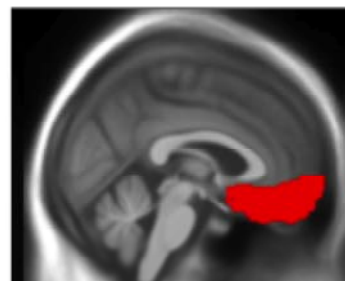
The five regions of interest (ROI) selected for deriving mean fluorodeoxyglucose metabolism. ROIs were delineated using the Wake Forest Pick Atlas (<http://fmri.wfubmc.edu/software/PickAtlas>).



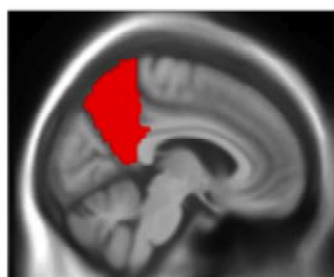
Lateral Parietal



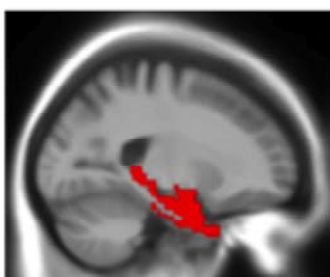
Hippocampus



Ventral PFC



Precuneus + PCC

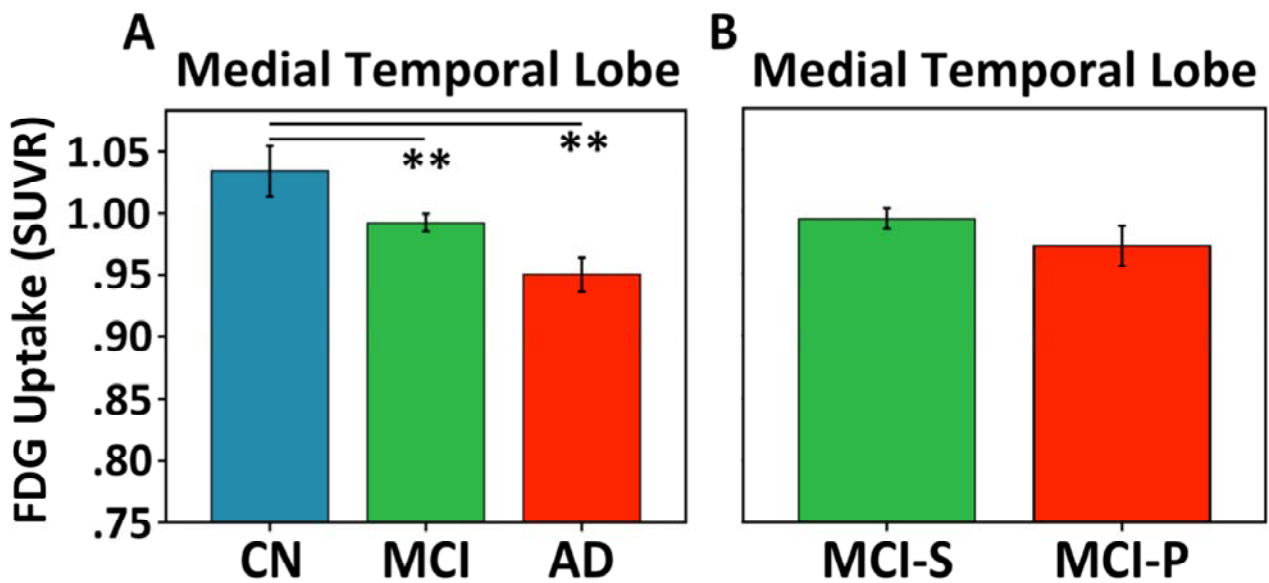


Medial Temporal Lobe

SUPPLEMENTARY DATA

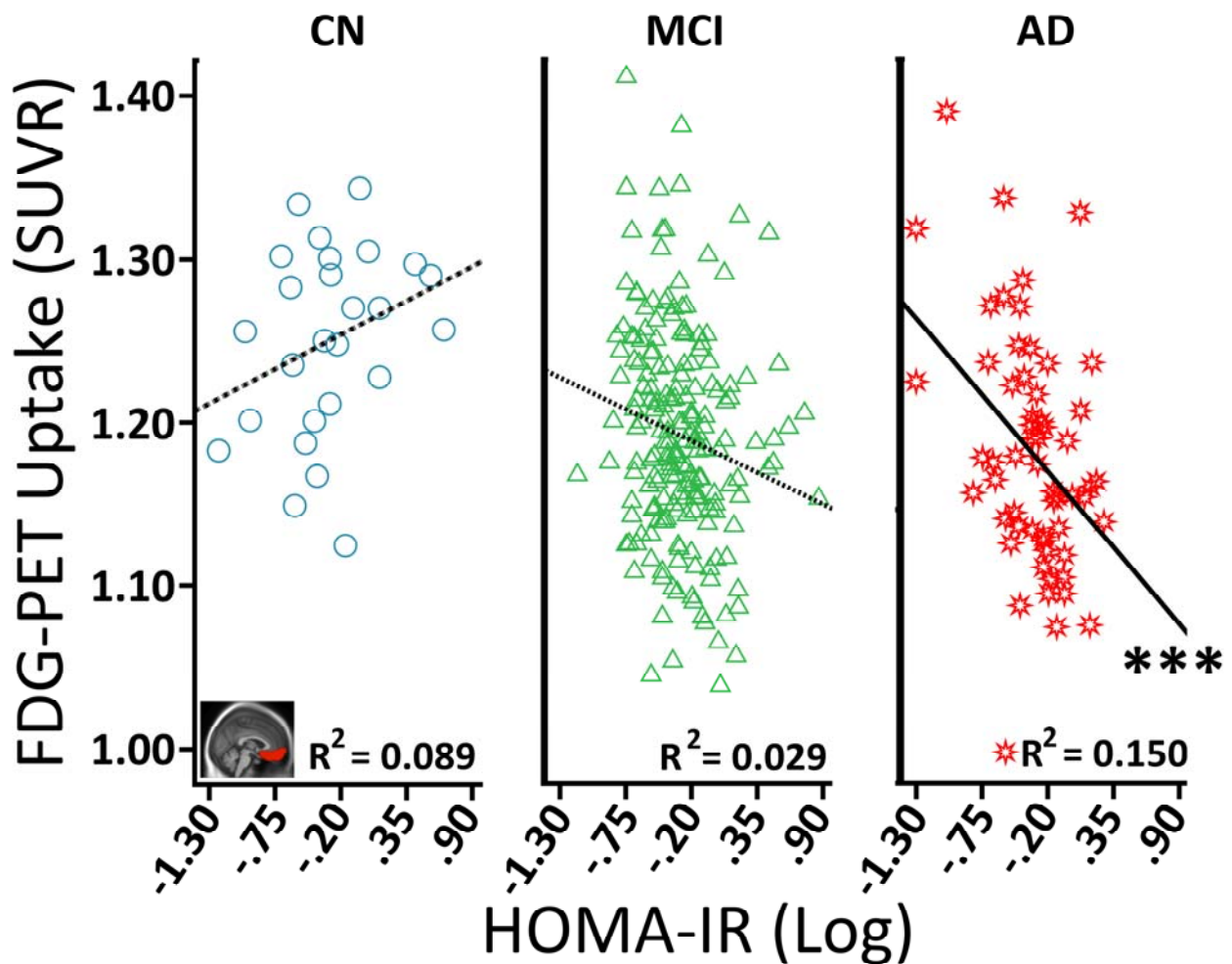
Supplementary Figure 2. Clinical Diagnosis and FDG-PET Uptake

The main effect of clinical diagnosis on mean fluorodeoxyglucose (FDG) metabolism in medial temporal lobe at baseline (A), or for MCI participants at 24 months (B). AD = Alzheimer's disease; CN = cognitively normal; FDG-PET= FDG Positron Emission Tomography; MCI = Mild Cognitive Impairment; MCI-P = progressive MCI; MCI-S = stable MCI; SUVR = Standardized Uptake Volume Ratio. ** = $p \leq .01$.



SUPPLEMENTARY DATA

Supplementary Figure 3. HOMA-IR and vPFC FDG Uptake among Baseline Diagnosis Groups
Associations between HOMA-IR and ventral prefrontal cortex (vPFC) fluorodeoxyglucose (FDG) metabolism. The “blue circle,” “green triangle,” and “red star” symbols correspond respectively to cognitively normal (CN), Mild Cognitive Impairment (MCI), and Alzheimer’s disease (AD) participants. The R^2 value refers to the proportion of variance in FDG metabolism explained by HOMA-IR for a given group. Covariates included: age at baseline, sex, education, hyperglycemia status, Apolipoprotein E (ApoE) $\epsilon 4$ genotype, and mean frontal GM volume. FDG-PET = FDG Positron Emission Tomography; HOMA-IR = Homeostatic Model Assessment of Insulin Resistance; SUVR = Standardized Uptake Volume Ratio. *** = $p \leq .001$.



SUPPLEMENTARY DATA

Supplementary Figure 4. HOMA-IR and vPFC FDG Uptake in MCI Conversion

Associations between HOMA-IR and ventral prefrontal cortex (vPFC) fluorodeoxyglucose (FDG) metabolism. The “green star” and “red square” symbols correspond to Mild Cognitive Impairment (MCI) participants who either remained stable (MCI-S) or progressed to AD by 24 months after baseline (MCI-P). The R^2 value refers to the proportion of variance in FDG uptake and metabolism explained by HOMA-IR for a given group. Covariates included: age at baseline, sex, education, hyperglycemia status, Apolipoprotein E (ApoE) $\epsilon 4$ genotype, and mean frontal GM volume. FDG-PET = FDG Positron Emission Tomography; HOMA-IR = Homeostatic Model Assessment of Insulin Resistance; SUVR = Standardized Uptake Volume Ratio. * = $p \leq .05$.

